REPORT

Observation of coherent elastic neutrino-nucleus scattering

D. Akimov[1,2], J. B. Albert[3], P. An[4], C. Awe[4,5], P. S. Barbeau[4,5], B. Becker[6], V. Belov[1,2], A. Brown[4,7], A. Bolozdynya[2], B...
+ See all authors and affiliations

Science 03 Aug 2017:
eaao0990
DOI: 10.1126/science.aao0990

Abstract

The coherent elastic scattering of neutrinos off nuclei has eluded detection for four decades, even though its predicted cross-section is the largest by far of all low-energy neutrino couplings. This mode of interaction provides new opportunities to study neutrino properties, and leads to a miniaturization of detector size, with potential technological applications. We observe this process at a 6.7-sigma confidence level, using a low-background, 14.6-kg CsI[Na] scintillator exposed to the neutrino emissions from the Spallation Neutron Source (SNS) at Oak Ridge National Laboratory. Characteristic signatures in energy and time, predicted by the Standard Model for this process, are observed in high signal-to-background conditions. Improved constraints on non-standard neutrino interactions with quarks are derived from this initial dataset.

The characteristic most often associated with neutrinos is a very small probability of interaction with other forms of matter, allowing them to traverse astronomical objects while undergoing no energy loss. As a result, large targets (tons to tens of kilotons) are used for their detection. The discovery of a weak neutral current in neutrino interactions (***1***) implied that neutrinos were capable of coupling to quarks through the exchange of neutral Z bosons. Soon thereafter it was suggested that this mechanism should also lead to coherent interactions between neutrinos and all nucleons present in an atomic nucleus (***2***). This possibility would exist only as long as the momentum exchanged remained significantly smaller than the inverse of the nuclear size (**Fig. 1A**), effectively restricting the process to neutrino energies below a few tens of MeV. The enhancement to the probability of interaction (scattering cross-section) would however be very large when compared to interactions with isolated nucleons, approximately scaling with the square of the number of neutrons in the nucleus (***2***, ***3***). For heavy nuclei and sufficiently intense neutrino sources, this can lead to a dramatic reduction in detector mass, down to a few kilograms.

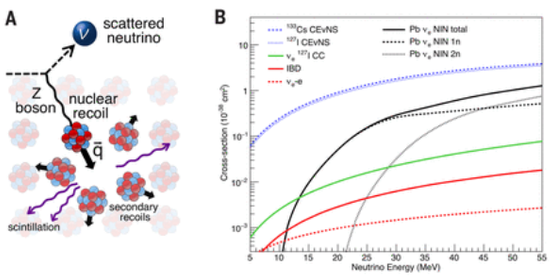

Download high-res image

Open in new tab

Download Powerpoint

Fig. 1 Neutrino interactions.

(**A**) Coherent Elastic Neutrino-Nucleus Scattering. For a sufficiently small momentum exchange (q) during neutral-current neutrino scattering ($qR < 1$, where R is the nuclear radius in natural units), a long-wavelength Z boson can probe the entire nucleus, and interact with it as a whole. An inconspicuous low-energy nuclear recoil is the only observable. However, the probability of neutrino interaction increases dramatically with the square of the number of neutrons in the target nucleus. In scintillating materials, the ensuing dense cascade of secondary recoils dissipates a fraction of its energy as detectable light. (**B**) Total cross-sections from CEvNS and some known neutrino couplings. Included are neutrino-electron scattering, charged-current (CC) interaction with iodine, and inverse beta decay (IBD). Because of their similar nuclear masses, cesium and iodine respond to CEvNS almost identically. The present CEvNS measurement involves neutrino energies in the range ~16-53 MeV, the lower bound defined by the lowest nuclear recoil energy measured (fig. S9), the upper bound by SNS neutrino emissions (fig. S2). The cross-section for neutrino-induced neutron (NIN) generation following $^{208}Pb(\nu_e,e^-\,xn)$ is also shown. This reaction, originating in lead shielding around the detectors, can generate a potential beam-related background affecting CEvNS searches. The cross-section for CEvNS is more than two orders of magnitude larger than for IBD, the mechanism employed for neutrino discovery (***35***).

Coherent elastic neutrino-nucleus scattering (CEvNS) has evaded experimental demonstration for forty-three years following its first theoretical description. This is somewhat surprising, in view of the magnitude of its expected cross-section relative to other tried-and-tested neutrino couplings (**Fig. 1B**), and of the availability of suitable neutrino sources: solar, atmospheric and terrestrial, supernova bursts, nuclear reactors, spallation facilities, and certain radioisotopes (***3***). This delay stems from the difficulty in detecting the low-energy (few keV) nuclear recoil produced as the single outcome of the interaction. Compared to a minimum ionizing particle of the same energy, a recoiling nucleus has a diminished ability to generate measurable scintillation or ionization in common radiation detector materials. This is exacerbated by a trade-off between the enhancement to the CEvNS cross-section brought about by a large nuclear mass, and the smaller maximum recoil energy of a heavy target nucleus.

The interest in CEvNS detection goes beyond completing the picture of neutrino couplings predicted by the Standard Model of particle interactions. In the time since its description, CEvNS has been suggested as a tool to expand our knowledge of neutrino properties. These studies include searches for sterile neutrinos (***4***–***6***), a neutrino magnetic moment (***7***, ***8***), non-standard interactions mediated by new particles (***9***–***11***), probes of nuclear structure (***12***), and improved constraints on the value of the weak nuclear charge (***13***). In addition to these, the reduction in neutrino detector mass may lead to a number of technological applications (***14***), such as non-intrusive nuclear reactor monitoring (***15***). CEvNS is also expected to dominate neutrino transport in neutron stars, and during stellar collapse (***16***–***18***). Direct searches for Weakly Interacting Massive Particles (WIMPs), presently favored dark matter candidates, rely on the same untested coherent enhancement to the WIMP-nucleus scattering cross-section, and will soon be limited by an irreducible CEvNS background from solar and atmospheric neutrinos (***19***). The importance of this process has generated a broad array of proposals for potential CEvNS detectors: superconducting devices (***3***), cryogenic detectors (***20***–***22***), modified semiconductors (***23***–***25***), noble liquids (***26***–***30***), and inorganic scintillators (***31***), among others.

The Spallation Neutron Source (SNS) at Oak Ridge National Laboratory generates the most intense pulsed neutron beams in the world, produced by the interactions of accelerator-driven high-energy (~1 GeV) protons striking a mercury target. These beams serve an array of neutron-scattering instruments, and a cross-disciplinary community of users. Spallation sources are known to simultaneously create a significant yield of neutrinos, generated when pions, themselves a byproduct of proton interactions in the target, decay at rest. The resulting low neutrino energies are favorable for CEvNS detection (***3***, ***32***, ***33***). Three neutrino flavors are produced (prompt muon neutrinos ν_μ, delayed electron neutrinos ν_e, and delayed muon anti-neutrinos $\bar{\nu}_\mu$), each with characteristic energy and time distributions (fig. S2), and all having a similar CEvNS cross-section for a given energy. During beam operation, approximately 5×10^{20} protons-on-target (POT) are delivered per day, each proton returning ~0.08 isotropically-emitted neutrinos per flavor. An attractive feature is the pulsed nature of the emission: 60 Hz of ~1 μs-wide POT spills. This allows us to isolate the steady-state environmental backgrounds affecting a CEvNS detector from the neutrino-induced signals, which should occur within ~10 μs windows following POT triggers. Similar time windows preceding the triggers can be inspected to obtain information about the nature and rate of steady-state backgrounds, which can then be subtracted (***31***, ***34***). A facility-wide 60 Hz trigger signal is provided by the SNS, at all times.

As large as this neutrino yield may seem, prompt neutrons escaping the iron and steel shielding monolith surrounding the mercury target (**Fig. 2**) would swamp a CEvNS detector sited at the SNS instrument bay. Neutron-induced nuclear recoils would largely dominate over neutrino-induced recoils, making experimentation impossible. This led to a systematic investigation of prompt neutron fluxes within the SNS facility (***34***). A basement corridor, now dubbed the "neutrino alley" was found to offer locations with more than 12 m of additional void-free neutron-moderating materials (concrete, gravel) in the line-of-sight to the SNS target monolith. An overburden of 8 m of water equivalent (m.w.e.) provides an additional reduction in backgrounds associated with cosmic rays. The CsI[Na] CEvNS detector and shielding described next were installed in the corridor location nearest to the SNS target (**Fig. 2**).

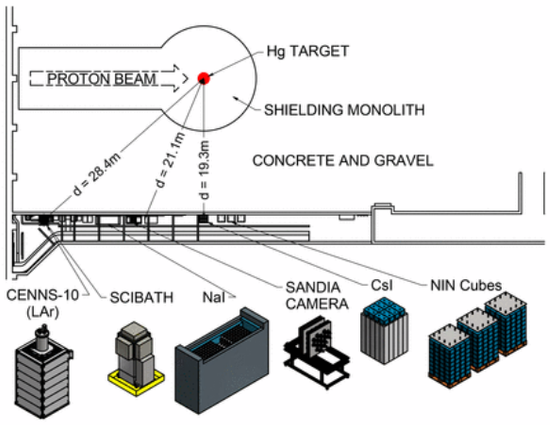

Fig. 2
COHERENT detectors populating the "neutrino alley" at the SNS (*34*).

Locations in this basement corridor profit from more than 19 m of continuous shielding against beam-related neutrons, and a modest 8 m.w.e. overburden able to reduce cosmic-ray induced backgrounds, while sustaining an instantaneous neutrino flux as high as 1.7×10^{11} ν_μ / cm^2 s.

Download high-res image
Open in new tab
Download Powerpoint

The advantages of sodium-doped CsI as a CEvNS detection material, its characterization for this application, and background studies using a 2 kg prototype are described in (***31***). Heavy cesium and iodine nuclei provide large cross-sections, and nearly-identical response to CEvNS (**Fig. 1B**), while generating sufficient scintillation for the detection of nuclear recoil energies down to a few keV. We performed supplementary calibrations of the final 14.6 kg CsI[Na] crystal before its installation at the SNS, as well as studies of the scintillation response to nuclear

recoils in the relevant energy region (*34*). In addition to these, an initial dedicated experiment was performed at the chosen detector location, measuring the very small flux of prompt neutrons able to reach this position, and constraining the maximum contribution from the neutrino-induced neutron (NIN) background that can originate in lead shielding surrounding the detector (**Fig. 1B**) (*34*). The conclusion from this measurement was that a CEvNS signal should largely dominate over beam-related backgrounds. The level of steady-state environmental backgrounds achieved in the final crystal slightly improved on expectations based on the prototype in (*31*), mostly thanks to refinements in data analysis, and to the presence of additional shielding. Further information about the experimental setup is provided in (*34*).

Figure 3 displays our main result, derived from fifteen months of accumulated live-time (fig. S1). When comparing CsI[Na] signals occurring before POT triggers, and those taking place immediately after, we observe a high-significance excess in the second group of signals, visible in both the energy spectrum and the distribution of signal-arrival times. This excess appears only during times of neutrino production ("Beam ON" in the figure). The excess follows the expected CEvNS signature very closely, containing only a minimal contamination from beam-associated backgrounds (*34*). NINs have a negligible contribution, even smaller than that from prompt neutrons, which is shown in the figure. The formation of the excess is strongly correlated to the instantaneous power on target (fig. S14). All neutrino flavors emitted by the SNS contribute to reconstructing the excess, as expected from a neutral current process. Stacked histograms in **Fig. 3** display the Standard Model CEvNS predictions for prompt ν_μ and delayed ν_e, emissions. Consistency with the Standard Model is observed at the one-sigma level (134 ± 22 events observed, 173 ± 48 predicted). A 2-D (energy, time) profile maximum likelihood fit favors the presence of CEvNS over its absence at the 6.7-sigma level (fig. S13). Further details and a discussion of uncertainties are provided in (*34*), together with similar results from a parallel analysis (fig. S11).

Download high-res image
Open in new tab
Download Powerpoint

Fig. 3
Observation of Coherent Elastic Neutrino-Nucleus Scattering.

Shown are residual differences (datapoints) between CsI[Na] signals in the 12 μs following POT triggers, and those in a 12-μs window before, as a function of their **(A)** energy (number of photoelectrons detected), and of **(B)** event arrival time (onset of scintillation). Steady-state environmental backgrounds contribute to both groups of signals equally, vanishing in the subtraction. Error bars are statistical. These residuals are shown for 153.5 live-days of SNS inactivity ("Beam OFF") and 308.1 live-days of neutrino production ("Beam ON"), over which 7.48 GWhr of energy (~1.76×10^{23} protons) was delivered to the mercury target. Approximately 1.17 photoelectrons are expected per keV of cesium or iodine nuclear recoil energy (*34*). Characteristic excesses closely following the Standard Model CEvNS prediction (histograms) are observed for periods of neutrino production only, with a rate correlated to instantaneous beam power (fig. S14).

Figure 4 shows an example of CEvNS applications: improved constraints on non-standard interactions between neutrinos and quarks, caused by new physics beyond the Standard Model (*9*–*11*). These are extracted from the maximum deviation from Standard Model CEvNS predictions allowed by the present dataset (*34*), using the parametrization in (*30*, *33*).

Download high-res image

Fig. 4 Constraints on non-standard neutrino-quark interactions.

Open in new tab

Download Powerpoint

Blue region: values allowed by the present data set at 90% C.L. (< 4.6) in space. These quantities parametrize a subset of possible non-standard interactions between neutrinos and quarks, where = 0,0 corresponds to the Standard Model of weak interactions, and indices denote quark flavor and type of coupling. The gray region shows an existing constraint from the CHARM experiment (***34***).

Data-taking continues, with neutrino production expected to increase this summer by up to 30%, compared to the average delivered during this initial period. In addition to CsI[Na], the COHERENT collaboration presently operates a 28 kg single-phase liquid argon (LAr) detector, 185 kg of NaI[Tl] crystals, and three modules dedicated to the study of NIN production in several targets (**Fig. 2**). Presently planned expansion includes a ~1 ton LAr detector with nuclear/electron recoil discrimination capability, an already-in-hand 2 ton NaI[Tl] array simultaneously sensitive to sodium CEvNS and charged-current interactions in iodine (**Fig. 1B**), and p-type point contact germanium detectors (***24***) with sub-keV energy threshold. We intend to pursue the new neutrino physics opportunities provided by CEvNS using this ensemble.

Supplementary Materials

www.sciencemag.org/cgi/content/full/science.aao0990/DC1

Supplementary Text

Figs. S1 to S14

References (***36***–***84***)

↵# The collaboration consists of all listed authors. There are no additional collaborators.

References and Notes

1. ↵ F. J. Hasert, S. Kabe, W. Krenz, J. Von Krogh, D. Lanske, J. Morfin, K. Schultze, H. Weerts, G. H. Bertrand-Coremans, J. Sacton, W. Van Doninck, P. Vilain, U. Camerini, D. C. Cundy, R. Baldi, I. Danilchenko, W. F. Fry, D. Haidt, S. Natali, P. Musset, B. Osculati, R. Palmer, J. B. M. Pattison, D. H. Perkins, A. Pullia, A. Rousset, W. Venus, H. Wachsmuth, V. Brisson, B. Degrange, M. Haguenauer, L. Kluberg, U. Nguyen-Khac, P. Petiau, E. Belotti, S. Bonetti, D. Cavalli, C. Conta, E. Fiorini, M. Rollier, B. Aubert, D. Blum, L. M. Chounet, P. Heusse, A. Lagarrigue, A. M. Lutz, A. Orkin-Lecourtois, J. P. Vialle, F. W. Bullock, M. J. Esten, T. W. Jones, J. McKenzie, A. G. Michette, G. Myatt, W. G. Scott, Observation of neutrino-like interactions without muon or electron in the Gargamelle neutrino experiment. *Phys. Lett. B* **46**, 138–140 (1973). doi:10.1016/0370-2693(73)90499-1 CrossRef Google Scholar

2. ↵ D. Z. Freedman, Coherent effects of a weak neutral current. *Phys. Rev. D* **9**, 1389–1392 (1974). doi:10.1103/PhysRevD.9.1389 CrossRef Google Scholar

3. ↵ A. Drukier, L. Stodolsky, Principles and applications of a neutral-current detector for neutrino physics and astronomy. *Phys. Rev. D* **30**, **2295–2309** (1984). doi:10.1103/PhysRevD.30.2295 CrossRef Google Scholar

4. ↵ A. J. Anderson, J. M. Conrad, E. Figueroa-Feliciano, C. Ignarra, G. Karagiorgi, K. Scholberg, M. H. Shaevitz, J. Spitz, Measuring active-to-sterile neutrino oscillations with neutral current coherent neutrino-nucleus scattering. *Phys. Rev. D* **86**, 013004 (2012). doi:10.1103/PhysRevD.86.013004 CrossRef Google Scholar

5. B. Dutta, Y. Gao, A. Kubik, R. Mahapatra, N. Mirabolfathi, L. E. Strigari, J. W. Walker, Sensitivity to oscillation with a sterile fourth generation neutrino from ultralow threshold neutrino-nucleus coherent scattering. *Phys. Rev. D* **94**, 093002 (2016). doi:10.1103/PhysRevD.94.093002 CrossRef Google Scholar

6. ↵ T. S. Kosmas, D. K. Papoulias, M. Tórtola, J. W. F. Valle, Probing light sterile neutrino signatures at reactor and spallation neutron source neutrino experiments. **https://arxiv.org/abs/1703.00054** (2017).

7. ↵ A. C. Dodd, E. Papageorgiu, S. Ranfone, The effect of a neutrino magnetic moment on nuclear excitation processes. *Phys. Lett. B* **266**, 434–438 (1991). doi:10.1016/0370-2693(91)91064-3 CrossRef Google Scholar

8. ↵ T. S. Kosmas, O. G. Miranda, D. K. Papoulias, M. Tórtola, J. W. F. Valle, Probing neutrino magnetic moments at the spallation neutron source facility. *Phys. Rev. D* **92**, 013011 (2015). doi:10.1103/PhysRevD.92.013011 CrossRef Google Scholar

9. ↵ J. Barranco, O. G. Miranda, T. I. Rashba, Sensitivity of low energy neutrino experiments to physics beyond the Standard Model. *Phys. Rev. D* **76**, 073008 (2007). doi:10.1103/PhysRevD.76.073008 CrossRef Google Scholar

10. P. deNiverville, M. Pospelov, A. Ritz, Light new physics in coherent neutrino-nucleus scattering experiments. *Phys. Rev. D* **92**, 095005 (2015). doi:10.1103/PhysRevD.92.095005 CrossRef Google Scholar

11. ↵ B. Dutta, R. Mahapatra, L. E. Strigari, J. W. Walker, Sensitivity to Z-prime and nonstandard neutrino interactions from ultralow threshold neutrino-nucleus coherent scattering. *Phys. Rev. D* **93**, 013015 (2016). doi:10.1103/PhysRevD.93.013015 CrossRef Google Scholar

12. ↵ K. Patton, J. Engel, G. C. McLaughlin, N. Schunck, Neutrino-nucleus coherent scattering as a probe of neutron density distributions. *Phys. Rev. C* **86**, 024612 (2012). doi:10.1103/PhysRevC.86.024612 CrossRef Google Scholar

13. ↵ L. M. Krauss, Low-energy neutrino detection and precision tests of the Standard Model. *Phys. Lett. B* **269**, 407–411 (1991). doi:10.1016/0370-2693(91)90192-S CrossRef Google Scholar

14. ↵ L. Stodolsky, Some neutrino events of the 21st century. Paper presented at Neutrino Astrophysics, Ringberg Castle, Tegernsee, Germany, 20–24 October 1997. **https://arxiv.org/abs/astro-ph/9801320v1** (1998).

15. ↵ Y. Kim, Detection of antineutrinos for reactor monitoring. *Nucl. Eng. Technol.* **48**, 285–292 (2016). doi:10.1016/j.net.2016.02.001 CrossRef Google Scholar

16. ↵ J. R. Wilson, Coherent neutrino scattering and stellar collapse. *Phys. Rev. Lett.* **32**, 849–852 (1974). doi:10.1103/PhysRevLett.32.849 CrossRef Google Scholar

17. D. N. Schramm, W. D. Arnett, Neutral currents and supernovas. *Phys. Rev. Lett.* **34**, 113–116 (1975). doi:10.1103/PhysRevLett.34.113 CrossRef Google Scholar

18. ↵ D. Z. Freedman, D. N. Schramm, D. L. Tubbs, The weak neutral current and its effects in stellar collapse. *Annu. Rev. Nucl. Sci.* **27**, 167–207 (1977). doi:10.1146/annurev.ns.27.120177.001123 CrossRef Web of Science Google Scholar

19. ↵ J. Billard, E. Figueroa-Feliciano, L. Strigari, Implication of neutrino backgrounds on the reach of next generation dark matter direct detection experiments. *Phys. Rev. D* **89**, 023524 (2014). doi:10.1103/PhysRevD.89.023524 CrossRef Google Scholar

20. ↵ B. Cabrera, L. M. Krauss, F. Wilczek, Bolometric detection of neutrinos. *Phys. Rev. Lett.* **55**, 25–28 (1985). doi:10.1103/PhysRevLett.55.25pmid:10031671 CrossRef PubMed Web of Science Google Scholar

21. C. Braggio, G. Bressi, G. Carugno, E. Feltrin, G. Galeazzi, Massive silicon or germanium detectors at cryogenic temperature. *Nucl. Instrum. Methods Phys. Res. A* **568**, 412–415 (2006). doi:10.1016/j.nima.2006.06.008 CrossRef Google Scholar

22. ↵ J. A. Formaggio, E. Figueroa-Feliciano, A. J. Anderson, Sterile neutrinos, coherent scattering, and oscillometry measurements with low-temperature bolometers. *Phys. Rev. D* **85**, 013009 (2012). doi:10.1103/PhysRevD.85.013009 CrossRef Google Scholar

23. ↵ S. A. Golubkov, Y. B. Gurov, K. N. Gusev, N. N. Egorov, N. I. Zamyatin, S. L. Katulina, Y. F. Kozlov, K. A. Kon'kov, V. G. Sandukovsky, A. I. Sidorov, A. S. Starostin, Investigation of the

internal amplification effect on planar (p^+-n-n^+) structures made of high-resistivity silicon. *Instrum. Exp. Tech.* **47**, 799–808 (2004). doi:10.1023/B:INET.0000049703.01596.be CrossRef Google Scholar

24. ↵ P. S. Barbeau, J. I. Collar, O. Tench, Large-mass ultralow noise germanium detectors: Performance and applications in neutrino and astroparticle physics. *J. Cosmol. Astropart. Phys.* **09**, 009 (2007). doi:10.1023/B:INET.0000049703.01596.be CrossRef Google Scholar

25. ↵ A. Aguilar-Arevalo, X. Bertou, C. Bonifazi, M. Butner, G. Cancelo, A. Castaneda Vazquez, B. Cervantes Vergara, C. R. Chavez, H. Da Motta, J. C. D'Olivo, J. D. Anjos, J. Estrada, G. Fernandez Moroni, R. Ford, A. Foguel, K. P. Hernandez Torres, F. Izraelevitch, A. Kavner, B. Kilminster, K. Kuk, H. P. Lima Jr., M. Makler, J. Molina, G. Moreno-Granados, J. M. Moro, E. E. Paolini, M. S. Haro, J. Tiffenberg, F. Trillaud, S. Wagner, The CONNIE experiment. *J. Phys. Conf. Ser.* **761**, 012057 (2016). doi:10.1088/1742-6596/761/1/012057 CrossRef Google Scholar

26. ↵ C. J. Horowitz, K. J. Coakley, D. N. McKinsey, Supernova observation via neutrino-nucleus elastic scattering in the CLEAN detector. *Phys. Rev. D* **68**, 023005 (2003). doi:10.1103/PhysRevD.68.023005 CrossRef Google Scholar

27. A. Bondar, A. Buzulutskov, A. Grebenuk, D. Pavlyuchenko, R. Snopkov, Y. Tikhonov, V. A. Kudryavtsev, P. K. Lightfoot, N. J. C. Spooner, A two-phase argon avalanche detector operated in a single electron counting mode. *Nucl. Instrum. Methods Phys. Res. A* **574**, 493–499 (2007). doi:10.1016/j.nima.2007.01.090 CrossRef Google Scholar

28. D. Yu. Akimov, I. S. Alexandrov, V. I. Aleshin, V. A. Belov, A. I. Bolozdynya, A. A. Burenkov, A. S. Chepurnov, M. V. Danilov, A. V. Derbin, V. V. Dmitrenko, A. G. Dolgolenko, Yu. V. Efremenko, A. V. Etenko, M. B. Gromov, M. A. Gulin, S. V. Ivakhin, V. A. Kantserov, V. A. Kaplin, A. K. Karelin, A. V. Khromov, M. A. Kirsanov, S. G. Klimanov, A. S. Kobyakin, A. M. Konovalov, A. G. Kovalenko, V. I. Kopeikin, T. D. Krakhmalova, A. V. Kuchenkov, A. V. Kumpan, E. A. Litvinovich, G. A. Lukyanchenko, I. N. Machulin, V. P. Martemyanov, N. N. Nurakhov, D. G. Rudik, I. S. Saldikov, M. D. Skorokhatov, V. V. Sosnovtsev, V. N. Stekhanov, S. V. Sukhotin, V. G. Tarasenkov, G. V. Tikhomirov, O. Y. Zeldovich, Prospects for observation of neutrino-nuclear neutral current coherent scattering with two-phase xenon emission detector. *J. Instrum.* **8**, P10023 (2013). doi:10.1016/j.nima.2007.01.090 CrossRef Google Scholar

29. T. H. Joshi, S. Sangiorgio, A. Bernstein, M. Foxe, C. Hagmann, I. Jovanovic, K. Kazkaz, V. Mozin, E. B. Norman, S. V. Pereverzev, F. Rebassoo, P. Sorensen, First measurement of the ionization yield of nuclear recoils in liquid argon. *Phys. Rev. Lett.* **112**, 171303 (2014). doi:10.1103/PhysRevLett.112.171303pmid:24836233 CrossRef PubMed Google Scholar

30. ↵ S. J. Brice, R. L. Cooper, F. DeJongh, A. Empl, L. M. Garrison, A. Hime, E. Hungerford, T. Kobilarcik, B. Loer, C. Mariani, M. Mocko, G. Muhrer, R. Pattie, Z. Pavlovic, E. Ramberg, K. Scholberg, R. Tayloe, R. T. Thornton, J. Yoo, A. Young, A method for measuring coherent elastic neutrino-nucleus scattering at a far off-axis high-energy neutrino beam target. *Phys. Rev. D* **89**, 072004 (2014). doi:10.1103/PhysRevD.89.072004 CrossRef Google Scholar

31. ↵ J. I. Collar, N. E. Fields, M. Hai, T. W. Hossbach, J. L. Orrell, C. T. Overman, G. Perumpilly, B. Scholz, Coherent neutrino-nucleus scattering detection with a CsI[Na] scintillator at the SNS spallation source. *Nucl. Instrum. Methods Phys. Res. A* **773**, 56–65 (2015). doi:10.1016/j.nima.2014.11.037 CrossRef Google Scholar

32. ↵ F. T. Avignone III, Y. V. Efremenko, Neutrino-nucleus cross-section measurements at intense, pulsed spallation sources. *J. Phys. G* **29**, **2615–2628** (2003). doi:10.1088/0954-3899/29/11/012 CrossRef Google Scholar

33. ↵ K. Scholberg, Prospects for measuring coherent neutrino-nucleus elastic scattering at a stopped-pion neutrino source. *Phys. Rev. D* **73**, 033005 (2006). doi:10.1103/PhysRevD.73.033005 CrossRef Google Scholar

34. ↵ See supplementary materials.

35. ↵ C. L. Cowan Jr., F. Reines, F. B. Harrison, H. W. Kruse, A. D. McGuire, Detection of the free neutrino: A confirmation. *Science* **124**, 103–104 (1956). doi:10.1126/science.124.3212.103pmid:17796274 FREE Full Text Google Scholar

36. ↵ N. E. Fields, thesis, University of Chicago (2014).

37. Proteus, Chagrin Falls, Ohio. Crystal grown by Amcrys, Kharkov, Ukraine.

38. K. Nakamura, Y. Hamana, Y. Ishigami, T. Matsui, Latest bialkali photocathode with ultra high sensitivity. *Nucl. Instrum. Methods Phys. Res. A* **623**, 276–278 (2010). doi:10.1016/j.nima.2010.02.220 CrossRef Google Scholar

39. J. Amaré, S. Cebrián, C. Cuesta, E. García, C. Ginestra, M. Martínez, M. A. Oliván, Y. Ortigoza, A. Ortiz de Solórzano, C. Pobes, J. Puimedón, M. L. Sarsa, J. A. Villar, P. Villar, Cosmogenic radionuclide production in NaI[Tl] crystals. *J. Cosmol. Astropart. Phys.* **02**, 046 (2015). doi:10.1016/j.astropartphys.2009.11.002 CrossRef Google Scholar

40. Geant4; **http://geant4.cern.ch**.

41. H. W. Bertini, Intra-nuclear cascade calculation of the secondary nucleon spectra from nucleon-nucleus interactions in the energy range 340 to 2900 MeV and comparisons with experiment. *Phys. Rev.* **188**, 1711–1730 (1969). doi:10.1103/PhysRev.188.1711 CrossRef Google Scholar

42. R. E. Prael, H. Lichtenstein, *User Guide to LCS: the LAHET Code System* (Tech. Rep. LA-UR-89-3014, Los Alamos National Laboratory, 1989).

43. R. L. Burman, M. E. Potter, E. S. Smith, Monte Carlo simulation of neutrino production by medium-energy protons in a beam stop. *Nucl. Instrum. Methods Phys. Res. A* **291**, 621–633 (1990). doi:10.1016/0168-9002(90)90012-U CrossRef Google Scholar

44. R. L. Burman, A. C. Dodd, P. Plischke, Neutrino flux calculations for the ISIS spallation neutron facility. *Nucl. Instrum. Methods Phys. Res. A* **368**, 416–424 (1996). doi:10.1016/0168-9002(95)00627-3 CrossRef Google Scholar

45. R. L. Burman, A. C. Dodd, P. Plischke, Forschungszentrum Karlsruhe Report FZKA 559 (July 1995).

46. R. L. Burman, P. Plischke, Neutrino fluxes from a high-intensity spallation neutron facility. *Nucl. Instrum. Methods Phys. Res. A* **398**, 147–156 (1997). doi:10.1016/S0168-9002(97)00821-8 CrossRef Google Scholar

47. D. R. F. Cochran, P. N. Dean, P. A. M. Gram, E. A. Knapp, E. R. Martin, D. E. Nagle, R. B. Perkins, W. J. Shlaer, H. A. Thiessen, E. D. Theriot, Production of charged pions by 730-MeV protons from hydrogen and selected nuclei. *Phys. Rev. D* **6**, **3085–3116** (1972). doi:10.1103/PhysRevD.6.3085 CrossRef Google Scholar

48. J. F. Crawford, M. Daum, G. H. Eaton, R. Frosch, H. Hirschmann, R. Horisberger, J. W. McCulloch, E. Steiner, R. Hausammann, R. Hess, D. Werren, Measurement of cross sections and asymmetry parameters for the production of charged pions from various nuclei by 585-MeV protons. *Phys. Rev. C* **22**, 1184–1196 (1980). doi:10.1103/PhysRevC.22.1184 CrossRef Google Scholar

49. J. W. Norbury, L. W. Townsend, Parametrized total cross sections for pion production in nuclear collisions. *Nucl. Instrum. Methods Phys. Res. B* **254**, 187–192 (2007). doi:10.1016/j.nimb.2006.11.054 CrossRef Google Scholar

50. E. Ronchi, P.-A. Söderström, J. Nyberg, E. Andersson Sundén, S. Conroy, G. Ericsson, C. Hellesen, M. Gatu Johnson, M. Weiszflog, An artificial neural network based neutron-gamma discrimination and pile-up rejection framework for the BC-501 liquid scintillation detector. *Nucl. Instrum. Methods Phys. Res. A* **610**, 534–539 (2009). doi:10.1016/j.nima.2009.08.064 CrossRef Google Scholar

51. X. L. Luo, V. Modamio, J. Nyberg, J. J. Valiente-Dobón, Q. Nishada, G. de Angelis, J. Agramunt, F. J. Egea, M. N. Erduran, S. Ertürk, G. de France, A. Gadea, V. González, T. Hüyük, G. Jaworski, M. Moszyński, A. Di Nitto, M. Palacz, P.-A. Söderström, E. Sanchis, A. Triossi, R. Wadsworth, Test of digital neutron-gamma discrimination with four different photomultiplier tubes for the Neutron Detector Array (NEDA). *Nucl. Instrum. Methods Phys. Res. A* **767**, 83–91 (2014). doi:10.1016/j.nima.2014.08.023 CrossRef Google Scholar

52. N. Mascarenhas, J. Brennan, K. Krenz, P. Marleau, S. Mrowka, Results with the neutron scatter camera. *IEEE Trans. Nucl. Sci.* **56**, 1269–1273 (2009). doi:10.1109/TNS.2009.2016659 CrossRef Google Scholar

53. S. A. Pozzi, S. D. Clarke, W. J. Walsh, E. C. Miller, J. L. Dolan, M. Flaska, B. M. Wieger, A. Enqvist, E. Padovani, J. K. Mattingly, D. L. Chichester, P. Peerani, MCNPX-PoliMi for nuclear nonproliferation applications. *Nucl. Instrum. Methods Phys. Res. A* **694**, 119–125 (2012). doi:10.1016/j.nima.2012.07.040 CrossRef Google Scholar

54. V. V. Verbinski, W. R. Burrus, T. A. Love, W. Zobel, N. W. Hill, R. Textor, Calibration of an organic scintillator for neutron spectrometry. *Nucl. Instrum. Methods* **65**, 8–25 (1968). doi:10.1016/0029-554X(68)90003-7 CrossRef Web of Science Google Scholar

55. D. J. Ficenec, S. P. Ahlen, A. A. Marin, J. A. Musser, G. Tarlé, Observation of electronic excitation by extremely slow protons with applications to the detection of supermassive charged particles. *Phys. Rev. D* **36**, 311–314 (1987). doi:10.1103/PhysRevD.36.311pmid:9958052 CrossRef PubMed Google Scholar

56. Toolkit for Data Modeling with ROOT (RooFit); **https://root.cern.ch/roofit**.

57. R. Lazauskas, C. Volpe, Low-energy neutrino scattering measurements at future spallation source facilities. *J. Phys. G* **37**, 125101 (2010). doi:10.1088/0954-3899/37/12/125101 CrossRef Google Scholar

58. R. Lazauskas, C. Volpe, Corrigendum: Low-energy neutrino scattering measurements at future spallation source facilities. *J. Phys. G* **42**, 059501 (2015). doi:10.1088/0954-3899/42/5/059501 CrossRef Google Scholar

59. E. Kolbe, K. Langanke, Role of ν-induced reactions on lead and iron in neutrino detectors. *Phys. Rev. C* **63**, 025802 (2001). doi:10.1103/PhysRevC.63.025802 CrossRef Google Scholar

60. A. R. Samana, C. A. Bertulani, Detection of supernova neutrinos with neutrino-iron scattering. *Phys. Rev. C* **78**, 024312 (2008). doi:10.1103/PhysRevC.78.024312 CrossRef Google Scholar

61. M. S. Athar, S. Ahmad, S. K. Singh, Neutrino nucleus cross sections for low energy neutrinos at SNS facilities. *Nucl. Phys. A.* **764**, 551–568 (2006). doi:10.1016/j.nuclphysa.2005.09.017 CrossRef Google Scholar

62. N. Jovančević, M. Krmar, D. Mrda, J. Slivka, I. Bikit, Neutron induced background gamma activity in low-level Ge-spectroscopy systems. *Nucl. Instrum. Methods Phys. Res. A* **612**, 303–308 (2010). doi:10.1016/j.nima.2009.10.059 CrossRef Google Scholar

63. A. G. Wright, An investigation of photomultiplier background. *J. Phys. E* **16**, 300–307 (1983). doi:10.1088/0022-3735/16/4/014 CrossRef Google Scholar

64. C. Bhatia, B. Fallin, M. E. Gooden, C. R. Howell, J. H. Kelley, W. Tornow, C. W. Arnold, E. M. Bond, T. A. Bredeweg, M. M. Fowler, W. A. Moody, R. S. Rundberg, G. Rusev, D. J. Vieira, J. B. Wilhelmy, J. A. Becker, R. Macri, C. Ryan, S. A. Sheets, M. A. Stoyer, A. P. Tonchev, Dual-fission chamber and neutron beam characterization for fission product yield measurements using monoenergetic neutrons. *Nucl. Instrum. Methods Phys. Res. A* **757**, 7–19 (2014). doi:10.1016/j.nima.2014.03.022 CrossRef Google Scholar

65. P. R. Beck, S. A. Payne, S. Hunter, L. Ahle, N. J. Cherepy, E. L. Swanberg, Nonproportionality of scintillator detectors. V. Comparing the gamma and electron response. *IEEE Trans. Nucl. Sci.* **62**, 1429–1436 (2015). doi:10.1109/TNS.2015.2414357 CrossRef Google Scholar

66. W. Mengesha, T. D. Taulbee, B. D. Rooney, J. D. Valentine, Light yield non-proportionality of CsI[Tl], CsI[Na], and YAP. *IEEE Trans. Nucl. Sci.* **45**, 456–461 (1998). doi:10.1109/23.682426 CrossRef Google Scholar

67. H. Park, D. H. Choi, J. M. Choi, I. S. Hahn, M. J. Hwang, W. G. Kang, H. J. Kim, J. H. Kim, S. C. Kim, S. K. Kim, T. Y. Kim, Y. D. Kim, Y. J. Kwon, H. S. Lee, J. H. Lee, M. H. Lee, S. E. Lee, S. H. Noh, I. H. Park, E. S. Seo, E. Won, H. Y. Yang, M. S. Yang, I. Yu, Neutron beam test of CsI crystal for dark matter search. *Nucl. Instrum. Methods Phys. Res. A* **491**, 460–469 (2002). doi:10.1016/S0168-9002(02)01274-3 CrossRef Google Scholar

68. C. Guo, X. H. Ma, Z. M. Wang, J. Bao, C. J. Dai, M. Y. Guan, J. C. Liu, Z. H. Li, J. Ren, X. C. Ruan, C. G. Yang, Z. Y. Yu, W. L. Zhong, C. Huerta, Neutron beam tests of CsI[Na] and CaF_2[Eu] crystals for dark matter direct search. *Nucl. Instrum. Methods Phys. Res. A* **818**, 38–44 (2016). doi:10.1016/j.nima.2016.02.037 CrossRef Google Scholar

69. V. I. Tretyak, Semi-empirical calculation of quenching factors for ions in scintillators. *Astropart. Phys.* **33**, 40–53 (2010). doi:10.1016/j.astropartphys.2009.11.002 CrossRef Google Scholar

70. J. Barranco, O. G. Miranda, T. I. Rashba, Probing new physics with coherent neutrino scattering off nuclei. *J. High Energy Phys.* **12**, 021 (2005). doi:10.1016/0370-2693(85)90942-6 CrossRef Google Scholar

71. J. F. Beacom, W. M. Farr, P. Vogel, Detection of supernova neutrinos by neutrino-proton elastic scattering. *Phys. Rev. D* **66**, 033001 (2002). doi:10.1103/PhysRevD.66.033001 CrossRef Google Scholar

72. L. M. Sehgal, Differences in the coherent interactions of ν_e, ν_μ, and ν_τ. *Phys. Lett. B* **162**, 370–372 (1985). doi:10.1016/0370-2693(85)90942-6 CrossRef Google Scholar

73. S. R. Klein, J. Nystrand, Exclusive vector meson production in relativistic heavy ion collisions. *Phys. Rev. C* **60**, 014903 (1999). doi:10.1103/PhysRevC.60.014903 CrossRef Google Scholar

74. J. D. Lewin, P. F. Smith, Review of mathematics, numerical factors, and corrections for dark matter experiments based on elastic nuclear recoil. *Astropart. Phys.* **6**, 87–112 (1996). doi:10.1016/S0927-6505(96)00047-3 CrossRef Web of Science Google Scholar

75. O. Behnke, K. Kroninger, G. Schott, T. Schrorner-Sadenius, Ed., *Data Analysis in High Energy Physics* (Wiley-VCH, 2013).

76. I. M. Chakravarti, R. G. Laha, J. Roy, *Handbook of Methods of Applied Statistics* (Wiley, 1967).

77. I. Stancu, Low energy neutrino cross-section measurements at the SNS. *Nucl. Phys. B Proc. Suppl.* **155**, 251–253 (2006). doi:10.1016/j.nuclphysbps.2006.02.064 CrossRef Google Scholar

78. *Spallation Neutron Source Final Safety Assessment Document for Neutron Facilities*, Oak Ridge National Laboratory Report 102030102-ES0016-R03 (September 2011).

79. P. Coloma, T. Schwetz, Generalized mass ordering degeneracy in neutrino oscillation experiments. *Phys. Rev. D* **94**, 055005 (2016). doi:10.1103/PhysRevD.94.055005 CrossRef Google Scholar

80. P. Coloma, P. B. Denton, M. C. Gonzalez-Garcia, M. Maltoni, T. Schwetz, Curtailing the dark-side in non-standard neutrino interactions. *J. High Energy Phys.* **2017**, 116 (2005). doi:10.1103/PhysRevD.94.055005 CrossRef Google Scholar

81. S. Davidson, C. Pena-Garay, N. Rius, A. Santamaria, Present and future bounds on non-standard neutrino interactions. *J. High Energy Phys.* **03**, 011 (2003). doi:10.1103/PhysRevD.94.055005 CrossRef Google Scholar

82. G. L. Fogli, E. Lisi, A. Marrone, D. Montanino, A. Palazzo, Getting the most from the statistical analysis of solar neutrino oscillations. *Phys. Rev. D* **66**, 053010 (2002). doi:10.1103/PhysRevD.66.053010 CrossRef Google Scholar

83. J. Dorenbosch, J. V. Allaby, U. Amaldi, G. Barbiellini, F. Bergsma, A. Capone, W. Flegel, L. Lanceri, M. Metcalf, C. Nieuwenhuis, J. Panman, K. Winter, I. Abt, J. Aspiazu, F. W. Büsser, H. Daumann, P. D. Gall, T. Hebbeker, F. Niebergall, P. Schütt, P. Stähelin, P. Gorbunov, E. Grigoriev, V. Khovansky, A. Rosanov, A. Baroncelli, L. Barone, B. Borgia, C. Bosio, M. Diemoz, U. Dore, F. Ferroni, E. Longo, L. Luminari, P. Monacelli, F. De Notaristefani, R. Santacesaria, C. Santoni, L. Tortora, V. Valente, Experimental verification of the universality of electron-neutrino and muon-neutrino coupling to the neutral weak current. *Phys. Lett. B* **180**, 303–307 (1986). doi:10.1016/0370-2693(86)90315-1 CrossRef Google Scholar

84. ↵ D. Akimov, P. An, C. Awe, P. S. Barbeau, P. Barton, B. Becker, V. Belov, A. Bolozdynya, A. Burenkov, B. Cabrera-Palmer, J. I. Collar, R. J. Cooper, R. L. Cooper, C. Cuesta, D. Dean, J. Detwiler, A. G. Dolgolenko, Y. Efremenko, S. R. Elliott, A. Etenko, N. Fields, W. Fox, A. Galindo-Uribarri, M. Green, M. Heath, S. Hedges, D. Hornback, E. B. Iverson, L. Kaufman, S. R. Klein, A. Khromov, A. Konovalov, A. Kovalenko, A. Kumpan, C. Leadbetter, L. Li, W. Lu, Y. Melikyan, D. Markoff, K. Miller, M. Middlebrook, P. Mueller, P. Naumov, J. Newby, D. Parno, S. Penttila, G. Perumpilly, D. Radford, H. Ray, J. Raybern, D. Reyna, G. C. Rich, D. Rimal, D. Rudik, K. Scholberg, B. Scholz, W. M. Snow, V. Sosnovtsev, A. Shakirov, S. Suchyta, B. Suh, R. Tayloe, R. T. Thornton, I. Tolstukhin, K. Vetter, C. H. Yu, The COHERENT experiment at the spallation neutrino source. **https://arxiv.org/abs/1509.08702** (2015).

35. **Acknowledgments:** We acknowledge support from: the Alfred P. Sloan Foundation (BR2014-037), the Consortium for Nonproliferation Enabling Capabilities (DE-NA0002576), the Institute for Basic Science (Korea) (IBS-R017-G1-2017-a00), the National Science Foundation (PHY-1306942, PHY-1506357, PHY-1614545, HRD-1601174), Lawrence Berkeley National Laboratory Directed Research and Development funds, Russian Foundation for Basic Research (No. **17-02-01077**_a), the Russian Science Foundation in the framework of MEPhI Academic Excellence Project (contract 02.a03.21.0005, 27.08.2013), Sandia National Laboratories Directed Research and Development Exploratory Express Funds, Triangle Universities Nuclear Laboratory, the U.S. Department of Energy Office of Science (DE-SC0009824, DE-SC0010007, Early Career Award DE-SC0014249, DE-SC0014558), the U.S. Department of Energy's National Nuclear Security Administration Office of Defense, Nuclear Nonproliferation Research, and Development, and the University of Washington Royalty Research Fund (FA124183). Sandia National Laboratories is a multimission laboratory managed and operated by National Technology and Engineering Solutions of Sandia LLC, a wholly owned subsidiary of Honeywell International Inc. for the U.S. Department of Energy's National Nuclear Security Administration under contract DE-NA0003525. Pacific Northwest National Laboratory is operated by Battelle for the United States Department of Energy under Contract No. DE-AC05-76RL01830, where work was supported through awards from the National Consortium for Measurement and Signature Intelligence Research Program, and from the Intelligence Community Postdoctoral Research Fellowship Program. This work was supported in part by the Kavli Institute for Cosmological Physics at the University of Chicago through grant NSF PHY-1125897, and an endowment from the Kavli Foundation and its founder Fred Kavli. This work was sponsored by the Laboratory Directed Research and Development Program of Oak Ridge National Laboratory, managed by UT-Battelle, LLC, for the U. S. Department of Energy. It used resources of the Spallation Neutron Source, which is a DOE Office of Science User Facility. This material is based upon work supported by the U.S. Department of Energy, Office of Science, Office of High Energy Physics. This research used resources of the Oak Ridge Leadership Computing Facility, which is a DOE Office of Science User Facility. Raw experimental data are archived at its High Performance Storage System, which provides 263 TB of COHERENT dedicated storage. We are grateful for additional resources provided by the research computing centers at the University of Chicago, and Duke University.

View Abstract